TIDE- AND STORMDRIVEN SEDIMENT TRANSPORT ON THE INNER-SHELF ALONG THE DUTCH COAST

Jan W.H. van de Meene[1] and Leo C. van Rijn[1,2]

ABSTRACT

Based on field observations, this paper discusses the hydrodynamic processes dominating the sediment mobility and sediment transport directions in the inner-shelf along the Dutch coast. Sediment transport observations during fair-weather conditions were obtained with a Total Load Sampler, that was operated from a ship. The sediment transport processes under storm conditions were analyzed using instantaneous velocity and suspended sediment concentration data obtained with a stand-alone platform. These data allow for the determination of the contributions of the mean, low- and high-frequency oscillatory sediment fluxes to the total flux (e.g. Wright et al., 1991).

INTRODUCTION

The near-bed water and sediment motion on the inner-shelf along the Dutch coast during fair-weather and storm conditions were studied using a Total Load Sampler and a stand-alone instrumented tripod. The objective of the study was to obtain insight in the processes that dominate the sediment mobility in the study area under different conditions. The field experiments discussed here form part of a larger research program that aims at establishing the formation and maintenance of a set of linear sand banks found on the inner-shelf along the central part of the Dutch coast. This program is carried out within the framework of the large Dutch multi-disciplinary research project 'Coastal Genesis'.

[1] Institute for Marine and Atmospheric Research Utrecht (IMAU), Netherlands Centre for Coastal Research (NCK), Utrecht University, P.O. Box 80.115, 3508 TC Utrecht, The Netherlands.

[2] Delft Hydraulics, P.O. Box 152, 8300 AD Emmeloord, The Netherlands.

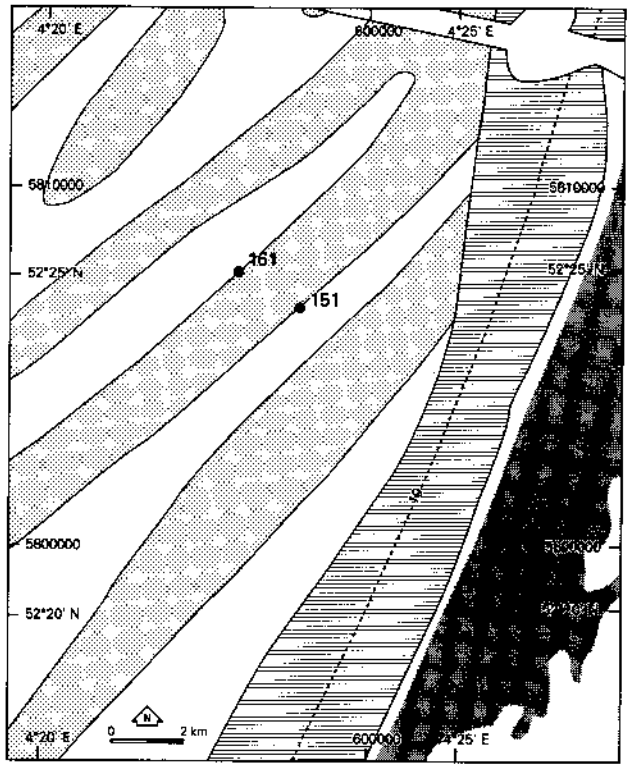

Figure 1 Location of the instrument deployments.

STUDY AREA

The inner-shelf along the central part of the Dutch coast is covered by a system of large linear sand banks (length 30 km, width 2-4 km, height 2-6 m), attached to the shoreface. The measurement sites were located near one of the ridges, in waterdepths between 14 and 16 m (Figure 1). The mean grain size of the sediments in the area is between 250 and 300 μm. The tidal range is between 1.5 and 2 m, giving near-bed tidal currents between 0.2 and 0.5 m/s. The mean annual wave height is 1.1 m, the wave height during typical winter storms (Bf. 8-10) is between 3 and 5 m. These conditions are typical for a mixed-energy shelf in a semi-enclosed sea. They indicate that sediment transport processes in the study area may be affected by both tidal currents and waves.

FIELD EXPERIMENTS

Sediment transport measurements during fair-weather conditions were done with a Total Load Sampler operated from a ship (Van Rijn and Gaweesh, 1992). This Total Load Sampler consists of a bedload trap and a set of intake nozzles, connected to pumps, to measure time-averaged suspended sediment concentrations. In addition, three current

meters (two Ott's and one electromagnetic flow meter) were mounted on the Total Load Sampler. The measurements were carried out on the top of one of the shoreface-connected ridges, between locations 151 and 161 (Figure 1), on 14 and 15 August 1990. The water depth at the location varied between 13 and 15 m. Maximum near bottom currents (0.45 m above the bed) were around 0.45 m/s, while depth-averaged currents obtained with an Elmar current meter reached values up to 0.8 m/s. During the measurements, the weather was fair, with a significant wave height of 0.3 and 0.8 m and a wave period of 4 s. The small scale morphology superimposed on the large ridges was determined from echosoundings and video-observations. The small scale bedforms consisted of megaripples with an average length of 10 m and an average height of 0.2-0.3 m and, superimposed on these small dunes, small scale ripples with an estimated length of 0.2 m and a height in the order of a few cm.

Sediment transport measurements during storm conditions were done with a stand-alone instrumented platform, built at the Department of Physical Geography, Utrecht University. An extensive description of this measurement frame (the 'EMF-frame') is given by Van de Meene (1994), and is summarized in the next section. The measurements presented here were obtained during an experiment in December 1991, at deployment site MP 161 (Figure 1). During the measurement period a couple of storms passed by with wind speeds up to 20 m/s (Bf. 8-9), significant wave heights up to 4 m, peak wave periods between 8 and 9 s and near bed wave orbital velocities up to 1.2 m/s.

THE EMF-FRAME: INSTRUMENTS AND CALIBRATIONS

Description of the measurement frame

The EMF-frame is a tripod with relatively thin and massive iron legs spaced wide apart (Figure 2). It is deployed in a classic U-mooring fashion, with a marking buoy used for retrieval. The Data Acquisition System (DAS) consists of a data logger (Campbell, model CR10, with a SM716 storage module) and a final data storage facility (a single board computer with 40MB harddisk). The data logger has been programmed to sample data in a burst mode. The power supply for the instrumentation consists of two sets of dry batteries, one set for the sensors and a separate set for the data logger and computer.

Electromagnetic flow meters (EMF's) were used to measure the instantaneous current velocity. These EMF's are two-axis flow meters, with a spherical head with a diameter of 4.0 cm. They have been produced by Delft Hydraulics. Suspended sediment concentrations were measured with optical backscatter sensors (OBS's) produced by D&A instruments (Downing et al., 1981). A pressure sensor (Keller) was used to register pressure fluctuations due to surface gravity waves and tidal water level variations (sampling frequency at 2 Hz.). An echosounder (HE-720 TS Seaview ultrasonic ranger) was mounted on the frames to monitor bed level changes. Tiltmeters were used to assess the position of the measurement frame relative to the sea bed and to verify whether the frames are positioned (approximately) level at the seabed. A compass (Plessy) was used to get the orientation of the electromagnetic flow meters relative to the magnetic north and also to record movements in the tripod.

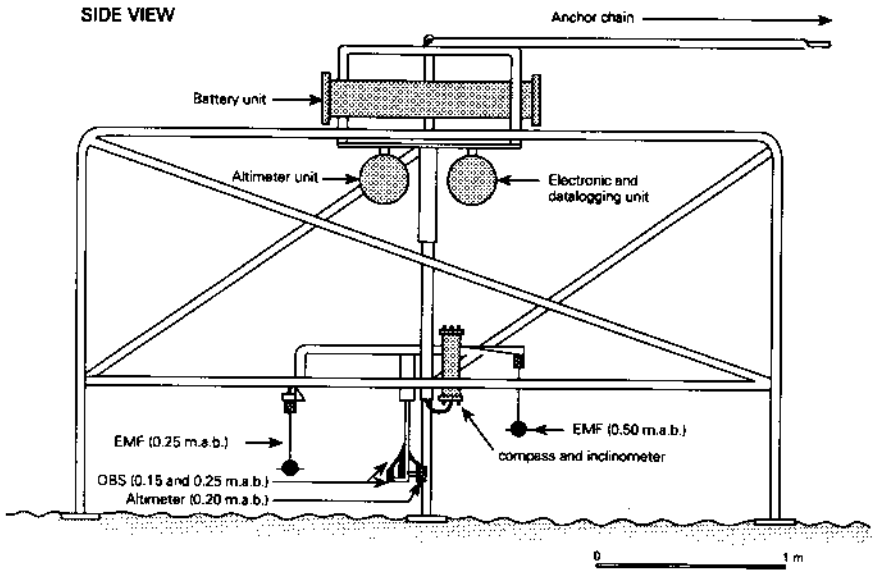

Figure 2 EMF-frame.

Calibration of validation of the EMF and OBS data

The electromagnetic flow meters were calibrated before and after the experiment in a towing tank at Delft Hydraulics. The calibrations were conducted for each axis (x and y) independently. The calibration curves are linear within the range of ± 2 m/s, with a high correlation coefficient ($R^2 > 0.999$). The variation in calibration curves for the sensors during different calibrations was negligible.

The OBS's were tested and calibrated in a circulation tank built at the Physical Geography Laboratory (Van de Meene, 1994). The sediments for these calibrations were obtained from the seabed at the deployment site and consisted of medium grained (d_{50} = 270 μm), well sorted sand. The calibrations were repeated three times. They show a linear trend over the entire range of concentrations (0-10 kg/m^3, linear fits with $R^2 >$ 0.999). The gain factors show little variation (coefficient of variation 3 to 6%), indicating that the calibration tank gives reproducible results.

In contrast with the gain factor of the OBS's, which can be determined accurately in the laboratory, the offset of the sensors during the measurements is difficult to establish. This offset consists of an electronic offset, inherent to the sensor, and a physical offset, caused by small background concentrations of mud, silt, or organic matter. It is not possible to distinguish between these two types of offset. Due to variations in background concentrations, the offset will vary in time, both in the calibration tank and in nature. The offset is ideally determined in the field, by in-situ calibrations. However, this was not possible in the present study, as the OBS's were mounted on a stand-alone frame. Alternatively, the total offset was estimated by the minimum reliable value encountered in each individual time-series. In each time-series, this minimum value was subtracted from

all observations. Doing this, it was implicitly assumed that the suspension process is intermittent, and that at least once during a burst a zero sand concentration was observed. Figure 7 reveals that this is a reasonable assumption, at least in a sandy inner-shelf environment. The absolute minimum in the OBS-series is always very close to the average of all local minima. This indicates that the absolute minimum forms a stable estimate for the base-level of the record.

The height of the OBS's above the bed may vary during an experiment, due to settling of the frame and migration of bedforms. Due to failure of the echosounder during the experiment, the exact measurement height of the OBS's is not known. To overcome this problem, an estimate of the height of the upper OBS was obtained using the degree of burial in the sea bed of the lower sensor. It was assumed that the amount of overflow data (missing values) registered with the lower OBS provided a measure for the extent to which this sensor was buried. With this assumption three different height classes could be distinguished: i. lower OBS above the sea bed (0-1% missing values); ii. lower OBS approximately at the sea bed (1-99% missing values); iii. lower OBS completely buried (100% missing values). Since the upper OBS was mounted 10 cm above the lower, these three height classes imply heights of the upper OBS: i. > 10 cm; ii. ≈ 10 cm; iii. < 10 cm. In all three cases the upper OBS had almost no missing values, indicating that it was positioned well above the bed.

Only the data from the upper OBS in height class 2 were selected for further analysis. Data falling in this height class have the best defined measurement height (approximately 0.1 m above the bed). Data from height class 1 appeared less accurate and less interesting, since they were obtained during much quieter conditions. As a result of these relatively quiet conditions, small background concentrations of organic matter, mud or algae may obscure the observed sand concentrations. The data falling in the third class were considered inaccurate due to the unknown but small height above the bed. Of a total of 74 usable bursts, 20 fell in height class 2. These data are discussed in the present paper.

FAIR-WEATHER SEDIMENT TRANSPORT

Data analysis

The bedload transport rates were determined using:

$$q_b = \frac{e(G_s - G_o)}{bT} \tag{1}$$

where q_b = bedload transport rate (kg/ms); G_s = dry weight of the total sand catch obtained with the bedload trap (kg); G_o = dry weight of the sand catch related to the initial and scooping effect (kg); b = width of the sampler mouth (=0.096 m) (m); T = sampling period (s); e = efficiency factor (-). The efficiency factor is assumed to be unity (Van Rijn et al., 1991). The dry weight (G_o) of the sand catch related to the initial and scooping effects was estimated by series of measurements with a zero-sampling period.

The suspended load transport (q_s) is defined as (cf. Van Rijn et al., 1991):

$$q_s = \int_a^h uc\,dz \tag{2}$$

where q_s = suspended load (kg/ms); a = thickness of the bedload layer (a = 0.04 m); h = water depth (m); u = flow velocity at height z above the bed (m/s); c = sand concentration at height z above the bed (kg/m^3).

A distinction between bedload and suspended load was made on practical grounds: the sediment caught in the bedload sampler is defined as bedload, the rest as suspended load. Tests were done in a laboratory flume to determine thickness of the layer of sediment that was trapped in the bedload bag. This height (a) above the bed appeared to be 0.04 m for low transport rates (filling percentage of the bag on average between 0 and 25 percent). The bedload transport is then the transport of the particles in a layer with thickness a = 0.04 m, the suspended load transport the transport of particles above that level. The thickness of the bedload layer corresponds reasonably well with the height of the observed small scale ripples. This suggests that the observed bedload transport occurs in the form of migration of these small scale ripples.

The velocity and concentration profile data measured by the impellor meters and by the suspended load sampler were extrapolated down to the height of the bedload layer (a = 0.04 m), using the three different extrapolation methods given by Van Rijn (1993). These methods gave comparable results, indicating that the obtained estimates are sufficiently reliable. The observed bedload and suspended load transport rates were compared with the prediction method of Van Rijn (1993).

Results and discussion

A selection of the current velocity, bedload and suspended load transport data is given in Figure 3 and 4 (15 August 1990, morning). The sampling period for the measurements presented here was 10 minutes. The median particle size of the bedload catches agreed well with the median grain size of the bed material (around 280 μm in both cases). The bedload transport rate is given in Figure 3. The measured transport rates were small and occurred only during a period of about 2 hours around maximum flow of the flood phase. Near-bed current velocities (0.45 m above the bed) were around 0.4 m/s during this period. The suspended sediment concentrations at z = 0.07, 0.11 and 0.15 m are given in Figure 4. The measured suspended sediment concentrations were very low, with a maximum value of 40 mg/l at 0.07 m above the bed. The depth-integrated suspended load transport rates were calculated using the measured sediment concentrations and current velocities (eqn. 2). These calculated suspended load transport rates are given in Figure 3 as well. The suspended load transport rates are slightly smaller than the bedload transport rates. The period during which sediment is transported in suspension is also shorter than the bedload transport period (1 hour). Based on this, it is concluded that bedload is dominant at low tidal velocities, whereas the total fair-weather transport is highly episodic.

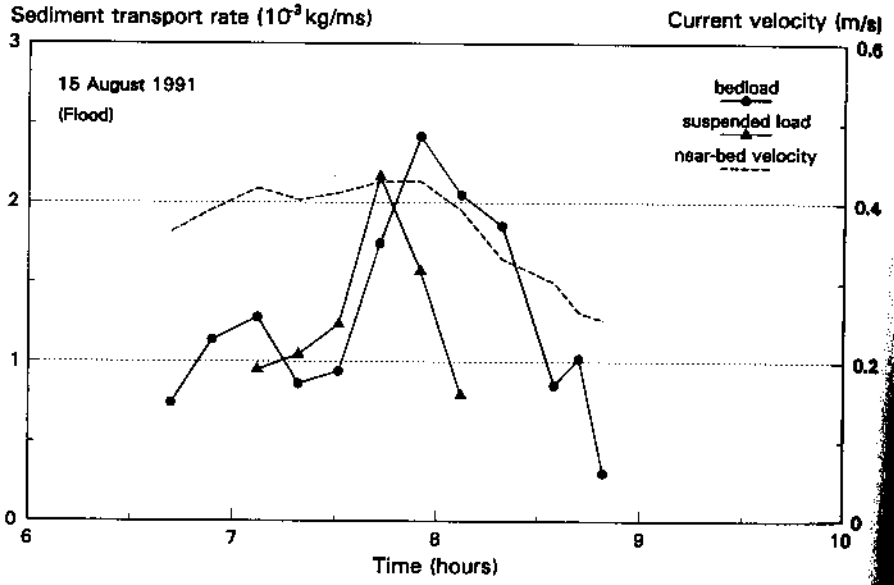

Figure 3 Near-bed current velocity, bed load and suspended load transport during springtide flood (15 August 1990).

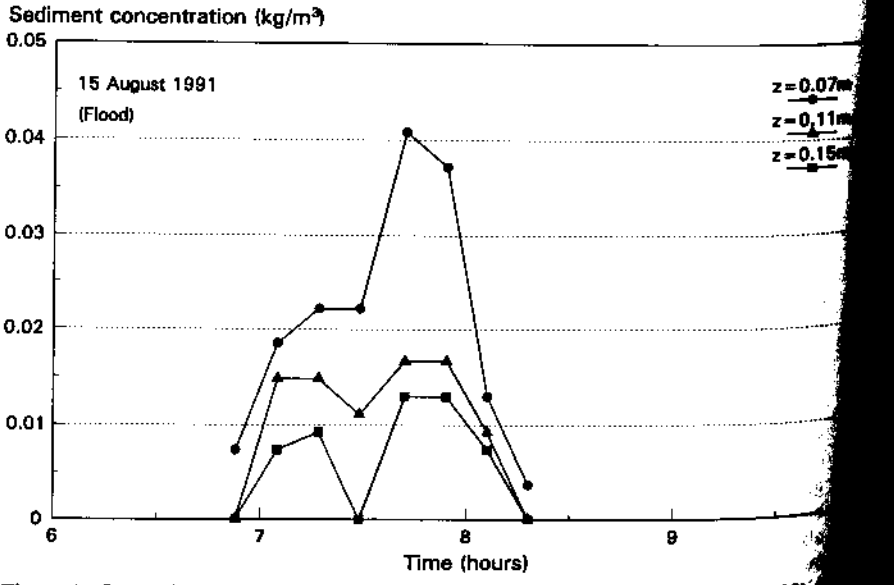

Figure 4 Suspended sediment concentrations during springtide flood (15 August 1990)

Table 1 Comparison measured and computed bed load and suspended load transport rates

$\bar{U}$ [1]	$\bar{U}_{corr}$ [2]	$\bar{U}_{0.5}$ [3]	Sediment transport rate			
			measured			computed
			(10^{-3}kg/ms)	n[4] (-)	vc[5] (-)	(10^{-3}kg/ms)
Bed load						
0.41	0.35	0.25	0.3 ± 0.6	3	1.0	0.001
0.56	0.48	0.35	0.8 ± 1.7	19	0.5	0.5
0.71	0.60	0.43	2.8 ± 2.1	9	0.3	2.8
Suspended load						
0.78	0.62	0.46	1.0 ± 0.5			3.6

Input parameters Transpor

h	= 14.4	(waterdepth)
d_{50}	= 276 μm	(median grainsize)
d_{90}	= 332 μm	(90% grainsize)
d_{ss}	= 276 μm	(suspended sediment size)
k_s	= 0.05 m	(current related roughness)
T	= 19° C	(water temperature)
Sa	= 30‰	(salinity)

1) Measured depth-averaged velocity
2) Depth-averaged velocity used as input for Transpor
3) Measured near-bed current velocity (0.5 m above the bed). The depth-averaged velocity used as input for Transpor has been chosen so that measured and calculated near-bed current velocities match.
4) Number of samples.
5) Variation coefficient ($= \sigma/\mu\sqrt{n}$, where σ, μ = standard deviation and average value of the measured sediment transport rate respectively; cf. Van de Meene, 1994)

For a comparison of the observed bedload and suspended load transport rates with the calculated transport rates using Van Rijn's (1993) transport model Transpor, the bedload measurements were lumped into three different near-bed velocity classes (0.2-0.3 m/s, 0.3-0.4 m/s, 0.4-0.46 m/s), while all suspended load measurements were lumped into one velocity class (0.42-0.5 m/s). The measured and computed bedload and suspended load transport rates for each velocity class are given in Table 1. The input conditions used for the Transpor calculations are given in Table 1 as well.

Sediment transport will occur when the effective bed shear stress τ_b' exceeds the critical bed shear stress $\tau'_{b,cr}$. Using the Shields diagram, initiation of motion for the given circumstances (mean water depth = 14.4 m; d_{50} = 276 μm; d_{90} = 332 μm) is predicted at a depth-averaged current velocity of 0.40 m/s (Van Rijn, 1993). The measurements (Table 1) show that this threshold velocity does not correspond with zero transport. This has been observed in laboratory experiments also (Van Rijn, 1993) and agrees with bedload observations in the river Waal (Van Rijn et al., 1991). It indicates that the method fails to predict the sediment transport rates at low current velocities.

correctly. At higher current velocities, the bedload sediment transport rates are predicted reasonably well. The suspended load transport rate is overpredicted by a factor 4.

SEDIMENT TRANSPORT DURING STORMS

Data analysis

The suspended sediment transport data were used to achieve a qualitative insight in the mechanisms that dominate the sediment transport processes during storms. The analysis followed the instantaneous approach, looking at the transport processes at an intra-wave time-scale. This concept has been applied in the nearshore zone by e.g. Jaffe et al. (1985), Osborne et al. (1990), and Davidson et al. (1993), and in the shoreface environment by Wright et al. (1991).

The instantaneous measurements of velocity and suspended sediment concentration can be decomposed into a mean and an oscillating component; the oscillating part, in addition, can be split into short and long periodic components:

$$u = \bar{u} + \tilde{u}_s + \tilde{u}_L \quad [m/s] \tag{3}$$

$$v = \bar{v} + \tilde{v}_s + \tilde{v}_L \quad [m/s] \tag{4}$$

$$c = \bar{c} + \tilde{c}_s + \tilde{c}_L \quad [kg/m^3] \tag{5}$$

where: u, v = cross- and along-bank wave orbital velocities (m/s); c = sediment concentration (kg/m^3); $\bar{u}$, $\bar{v}$, $\bar{C}$ = time-averaged values; $\tilde{u}_S$, $\tilde{v}_S$, $\tilde{C}_S$ = high-frequency oscillations; $\tilde{u}_L$, $\tilde{v}_L$, $\tilde{C}_L$ = low-frequency oscillations.

As a result, the total time-averaged cross- and along-bank sediment fluxes $<cu>$ and $<cv>$ can be split into a mean flux component and several oscillating flux components:

$$<uc> = \bar{u}\bar{c} + <\tilde{u}_s\tilde{c}_s> + <\tilde{u}_L\tilde{c}_L> + <\tilde{u}_s\tilde{c}_L> + <\tilde{u}_L\tilde{c}_s> \quad [kg/m^2s] \tag{6}$$

$$<vc> = \bar{v}\bar{c} + <\tilde{v}_s\tilde{c}_s> + <\tilde{v}_L\tilde{c}_L> + <\tilde{v}_s\tilde{c}_L> + <\tilde{v}_L\tilde{c}_s> \quad [kg/m^2s] \tag{7}$$

In the present study, the brackets $< >$ indicate time-averaging over 10 minutes. The long and short periodic components were obtained by low- and high-pass filtering the instantaneous time-series, with a cutoff frequency of 0.05 Hz. This is twice the maximum observed peak incident wave period. In total a set of 6 fluxes is obtained: a total flux, consisting of a mean and four oscillatory fluxes. The mean flux is, by definition, directed

in the direction of the mean current. In the inner-shelf environment, this mean current is a combination of tide, wind- and density-driven flows, with the Coriolis effect acting on all these currents. The short wave flux represents the net effect of the sediment fluxes induced by the incident wave orbital motion. This short wave flux may be directed with the propagation direction of the waves, when the waves are asymmetric, while it may be directed against the wave propagation direction, when strong vortex motions over steep ripples dominate, giving a net backward transport (e.g. Van Rijn, 1993). The long wave oscillatory flux is associated with the bound long waves, associated with grouped wind waves (e.g. Roelvink, 1993). The short-long wave interaction terms were found to be zero, indicating that $\tilde{u}_S$ and $\tilde{u}_L$ are uncorrelated with $\tilde{c}_L$ and $\tilde{c}_S$ respectively. The sediment fluxes, calculated according to equations 7 and 8 are represented by depicting the fluxes in x and y direction in vector diagrams.

The asymmetry ratio for the near-bed orbital velocity was defined by:

$$A_V = \frac{V_{s,crest}}{V_{s,crest} + V_{s,trough}} \tag{8}$$

where: A_v = asymmetry ratio (-); $V_{s,crest}$ = significant current velocity under the wave crest (onshore, m/s); $V_{s,trough}$ = significant current velocity under the wave troughs (m/s). This ratio equals 0.5 for symmetric waves and takes a value between 0.5 and 1 for (shoreward) asymmetric waves. Similarly, an asymmetry factor was defined for the oscillatory fluxes ($<u_S \cdot c_S>$ etc.).

Results

The asymmetry ratio's for the wave orbital velocities and for the oscillatory fluxes, as a function of $V_{s,crest}$, are given in Figure 5. The orbital velocity asymmetry ratio is between 0.50 and 0.55 and independent of $V_{s,crest}$ (Figure 5a). This indicates that waves were slightly asymmetrical during the observed storm conditions. The measured wave orbital velocities could be reproduced well with linear wave theory.

The oscillatory flux asymmetry increases with increasing peak velocity, albeit with considerable scatter (Figure 5b). The range of flux asymmetries varies between 0.25 and 0.75. Here, asymmetries < 0.5 indicate sediment fluxes directed against the propagation direction of the incident waves and asymmetries > 0.5 indicate fluxes directed with the incident waves. This corresponds with a seaward sediment flux component for an asymmetry ratio < 0.5 and a landward sediment flux component for an asymmetry ratio > 0.5. The transition between seaward and landward directed oscillatory fluxes is around $V_{s,crest} = 0.7$ m/s (Figure 5b).

A selection of vectorplots showing the measured sediment fluxes at 0.1 m above the bed during two different bursts, is given in Figure 6. In general, the mean fluxes $\bar{u}\cdot\bar{c}$ and $\bar{v}\cdot\bar{c}$ are dominant. This indicates that wave stirring and advection by the mean current is the dominant sediment transporting process. The short wave oscillatory fluxes are variable in magnitude and direction and may cause significant differences between the

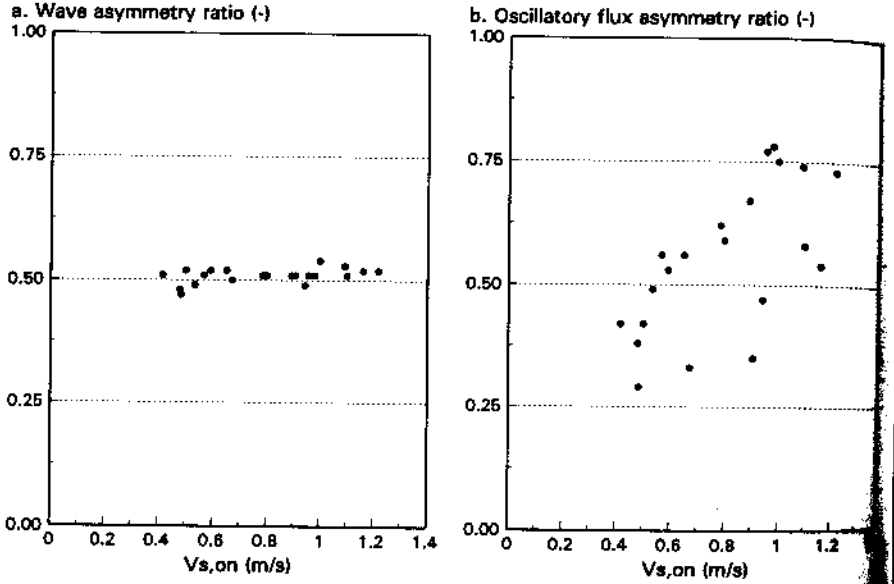

Figure 5 Asymmetry ratios as a function of $V_{s,on}$. a). wave orbital velocities; b). wave orbital fluxes.

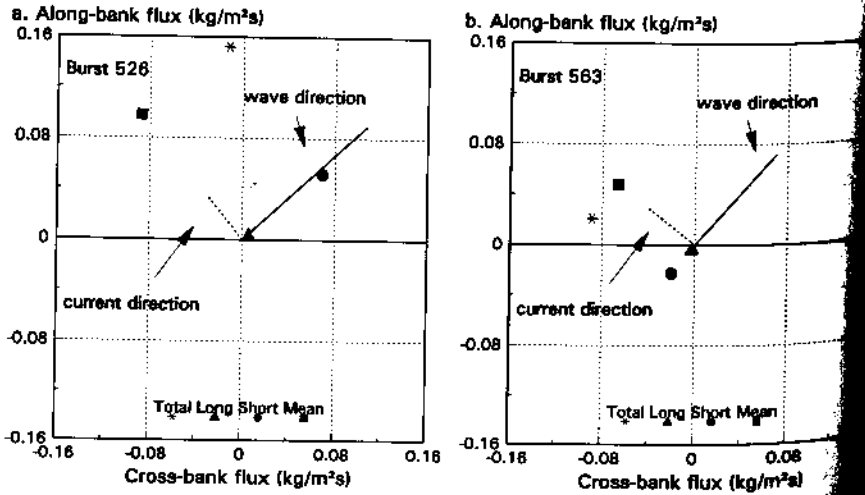

Figure 6 Vector plots of sediment fluxes. a). burst 526; b). burst 563. Dotted line represents current direction, solid line represents wave direction.

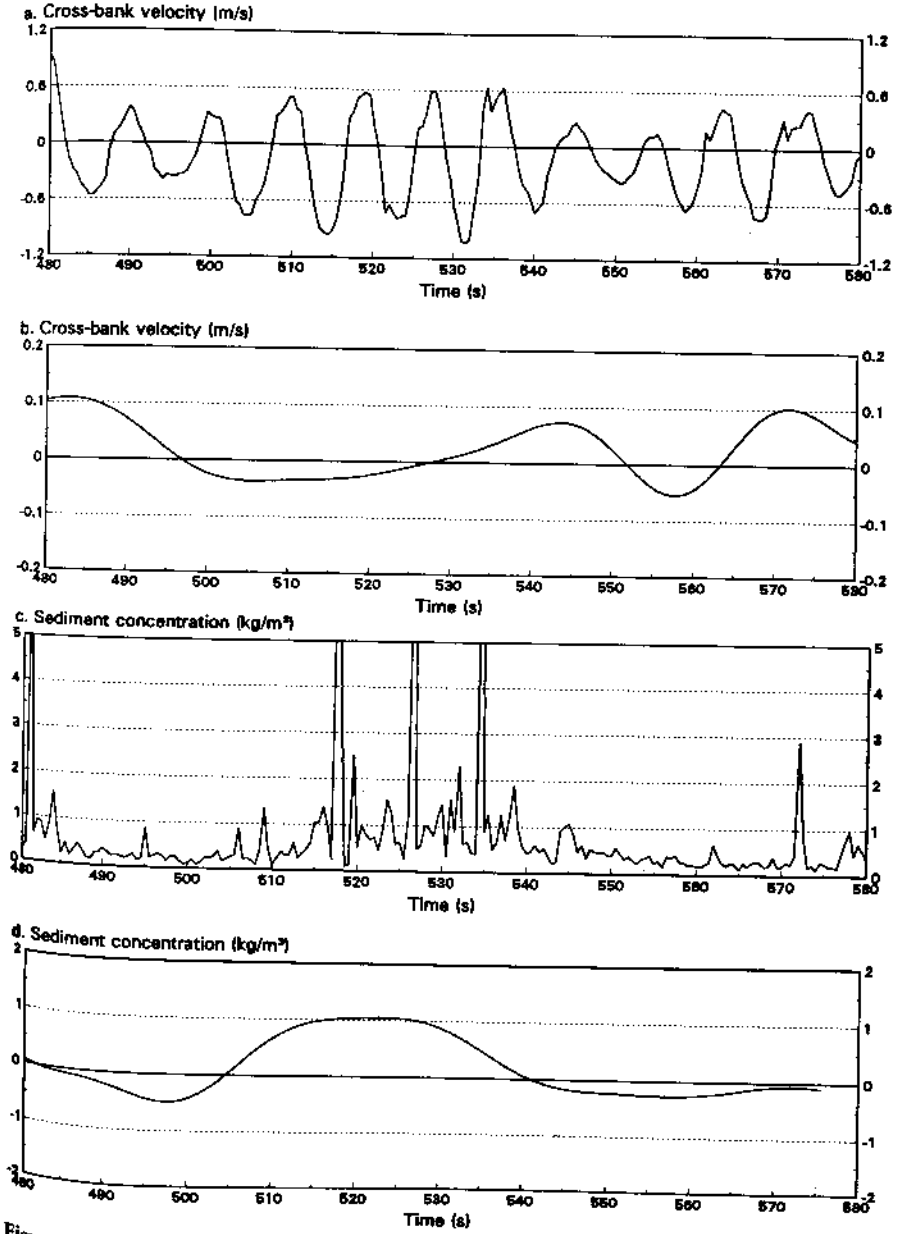

Figure 7 Detail of water and sediment motion during burst 526 (18 December 1991;

mean and the total sediment fluxes. The long wave oscillatory fluxes are always very small and may be neglected.

An example of the water and sediment motion is given in Figure 7. This figure shows a distinct groupiness of the waves, while the suspended sediment concentrations are clearly correlated with the wave groups. The fact that the long wave fluxes are negligibly small (Figure 6), indicates that there is no net sediment flux induced by these wave groups. Figure 7 shows the irregular and rapidly changing nature of the suspended sediment events. Peaks in sediment concentration are only partially correlated with peaks in wave orbital velocity. During one half-wave cycle more than one concentration peak may be observed. In addition, there are small phase-differences between the wave-orbital motion and the sediment concentration. During burst 526, the wave oscillatory fluxes were positive, directed landward, in the direction of the waves (Figure 6). In this case the largest suspension peaks occur during positive (shoreward) wave orbital velocities. Inspection of other time-series with positive wave oscillatory fluxes shows that the trend described above is valid in general; when the oscillatory flux is negative, the reverse applies. Small or zero oscillatory fluxes occur when the wave orbital velocity is relatively small.

The observed mean sediment concentrations at 0.1 m above the bed during typical storm conditions (U_{tide} = 0.6 m/s, H_s = 3 m, T_p = 7 s) was in the order of 0.4 kg/m^3. This value could be predicted well with Van Rijn's transport model (Van Rijn, 1993).

Discussion

The observed transition between landward directed oscillatory fluxes (directed with the incoming waves) and seaward directed fluxes (directed against the incoming waves), at wave orbital velocities around 0.7 m/s, may be related to the transition of a rippled bed towards a plane bed. Vortex shedding, induced by small ripples, may cause net seaward oscillatory fluxes (e.g. Van Rijn, 1993). Landward directed oscillatory fluxes may be related to (slightly) asymmetrical wave orbital velocities under plane-bed conditions.

The wave orbital velocity at which the transition from a rippled bed to plane bed conditions takes place is not very well defined (Van Rijn, 1993). The range, according to Dingler & Inman (1977), varies between 0.46 and 1.14 m/s, depending on the wave period and the grain size. Preceding flow conditions may also be important (hysteresis effects, Van Rijn, 1993). For grainsizes around 200-300 μm, Allen (1984) gives a value of 0.7 m/s, which is also the value adopted by Davidson et al., (1993) for their measurements. This value of 0.7 m/s corresponds well with the orbital velocities at which a transition is found between on- and offshore directed oscillatory fluxes in the Zandvoort data (Figure 5b). The Zandvoort data also suggest that some hysteresis effect may be important (Figure 5b). Unfortunately, detailed information on the bed topography during the measurements is lacking, so the assumed relationship between bed topography and oscillatory flux direction remains speculative. The results stress the importance of registering the bedforms during the measurements, although this is virtually impossible in practice, especially during storm conditions (Vincent et al., 1991).

Wright et al. (1991) have done an extensive study on sediment transport processes in the sandy shoreface environment along the east coast of U.S.A., in water depths generally around 10 m and with a maximum of 17 m. The measurements described here can be compared with their study; the measurement techniques in both studies are roughly similar.

Comparable with the data presented in this paper, Wright et al. (1991) find the mean sediment fluxes to be the most important contributor to the total sediment flux. They found this to be the case for a variety of different conditions, ranging from fair-weather to storms. Incident waves were found to be important for stirring up the sediment. As in the present study, oscillatory fluxes were directed onshore as well as offshore. According to Wright et al. (1991), this variety in direction may be explained by phase lags between u(t) and c(t), caused by the presence of small scale ripples. Low-frequency effects were measurable, but not dominant. Low-frequency fluxes were directed landward as well as seaward. Part of their data set covers a storm (dataset obtained near Duck, N.C. in 1985), allowing a more specific comparison with the data presented here. Their storm data were obtained at the shoreface at a water depth of 8 m. The significant wave height was between 1 and 1.4 m, the significant wave period around 8 s, while the observed wave orbital velocities were in the order of 1 m/s. These conditions were slightly quieter, but further reasonably comparable with the conditions under which the Zandvoort data were obtained. The median grainsize (d_{50}) of the bed material near Duck, N.C. was 125 μm, which is finer than the Zandvoort sediments (d_{50} around 270 μm).

There is good agreement between the results from both experiments. Although in both studies the mean sediment fluxes were dominant, the type of mean flow was different: during the Duck experiment the mean flow was dominated by seaward directed downwelling, while during the Zandvoort measurements the mean flow consisted of tidal and wind-driven currents. The sediment fluxes are of comparable magnitude, with mean sediment fluxes in the order of 0.02-0.50 kg/m^{2}s (Zandvoort) and 0.05-0.30 kg/m^{2}s (Duck), and oscillating fluxes in the order of 0-0.01 kg/m^{2}s (Zandvoort) and 0-0.04 kg/m^{2}s (Duck).

CONCLUSIONS

Sediment transport observations during spring tidal, fair-weather conditions have shown that the sediment transport rates under these conditions are very low and occur only during a period of about 2 hours around maximum tidal flow. Bedload transport is slightly dominant.

The sediment transport measurements during storm conditions have revealed a large variability in transport directions. Although the mean fluxes dominate the sediment mobility during storms, the contribution of short wave oscillatory fluxes to the total flux cannot be neglected. Long wave oscillatory fluxes are negligible.

Calculations with the Transpor model (Van Rijn, 1993) agree reasonably well with the observed sediment transport rates and suspended sediment concentrations, under fair-weather and under storm conditions.

ACKNOWLEDGEMENTS

This study was done within the framework of the Coastal Genesis Programme and was partly funded by the National Institute for Coastal and Marine Management (RIKZ) of the Ministry of Transport, Public Works and Water Management. Technical assistance for these measurements was provided by the Department of Physical Geography, Utrecht University. The crew of RV *Professor Lorentz* skilfully handled the instruments at sea.

REFERENCES

Allen, J.R.L. (1984). Sedimentary structures. Their characters and Physical basis. *Developments in Sedimentology*, 30. I: 593 pp, II: 663 pp. Elsevier Publisher B.V., Amsterdam.

Davidson, M.A., P.E. Russell, D.A. Huntley & J. Hardisty (1993). Tidal asymmetry in suspended sand transport on a macrotidal intermediate beach. *Marine Geology*, 110: 333-353.

Dingler, J.R. & D.L. Inman (1977). Wave-formed ripples in nearshore sands. *Proceedings 15th Conference on Coastal Engineering*, ASCE, New York: 2109-2126.

Downing, J.P., R.W. Sternberg & C.R.B. Lister (1981). New instrumentation for the investigation of sediment suspension processes in the shallow marine environment. *Marine Geology*, 42: 19-34.

Jaffe, B.E., R.W. Sternberg and A.H. Sallenger (1985). The role of suspended sediment in shore-normal beach profile changes. *Proceedings 19th Conference on Coastal Engineering*, ASCE, New York, 1983-1996.

Osborne, P.D., B. Greenwood & A.J. Bowen (1990). Cross-shore suspended sediment transport on a non-barred beach: the role of wind waves, infragravity waves and mean flows. *Proceedings of the Canadian Coastal Conference 1990*: 349-361.

Roelvink, J.A. (1993). Surf beat and its effect on cross-shore profiles. Thesis, Technical University Delft, 116 pp..

Van de Meene, J.W.H. (1994). The shoreface-connected ridges along the central Dutch coast. Ph.D-thesis. *KNAG/Netherlands Geographical Studies 174*, Utrecht, The Netherlands, 222 pp..

Van Rijn, L.C. (1993). Principles of sediment transport in rivers, estuaries and coastal seas. Aqua Publications, Amsterdam, The Netherlands.

Van Rijn, L.C., B. Kornman & B. Gehrels (1991). The Delft Nile Sampler. Bedload transport measurements in the river Waal. Report Q1300.02/h840.21. Delft Hydraulics, Delft, The Netherlands.

Van Rijn, L.C. and M. Gaweesh (1992). A new total load sampler. *Journal of Hydraulic Engineering*, Vol. 118, No. 112.

Vincent, C.E. & D.M. Hanes & A.J. Bowen (1991). Acoustic measurements of suspended sand on the shoreface and the control of concentration by bed roughness. *Marine Geology*, 96: 1-18.

Wright, L.D., J.D. Boon, S.C. Kim and J.H. List (1991). Modes of cross-shore transport on the shoreface of the Middle Atlantic Bight. *Marine Geology*, 96: 19-51.

SEDIMENT TRANSPORT MEASUREMENTS IN COMBINED WAVE-CURRENT FLOWS

I. Katopodi[1], J. S. Ribberink[2], P. Ruol[3] and C. Lodahl[4]

ABSTRACT: A series of experiments were carried out in the Large Oscillating Water Tunnel of Delft Hydraulics in the end of 1993. The aim of the investigation was to study the behaviour of the sediment and water flow in the wave-current boundary layer in the sheet flow regime. Four conditions with sinusoidal waves and net currents were realized. A selected part of the new experimental data is presented. The attention is focused on vertical profiles of time-averaged and time-dependent suspended sediment concentrations and velocities as well as net sediment transport rates.

INTRODUCTION

The understanding of the physical processes of the near-bed dynamics under the influence of waves and currents, crucial for an adequate prediction of the sea bed changes and coast line evolution, is very limited. The validity of the various mathematical models can hardly be assessed due to the low number of measurements available, especially at prototype scale (see Horikawa, 1988). Especially scarce are the measurements in the wave boundary layer near the sea bed.

The Large Oscillating Water Tunnel of Delft Hydraulics is a large scale experimental facility in which wave- and current-related near-bed flow and sediment transport phenomena can be simulated in the scale of nature (1:1). During the preceding years the tunnel became an important source of

1) Scientific Officer, Democritus University of Thrace, Department of Civil Engineering, 67100 Xanthi, Greece.
2) Senior Researcher, Delft Hydraulics, P.O. Box 152, 8300 AD Emmeloord, the Netherlands.
3) Researcher, University of Padova, Faculty of Engineering, Institute of Maritime Constructions, Via Ognissanti 39, 35129, Padova, Italy.
4) Ph.D student, Technical University of Denmark, ISVA, Building 115, Lyngby, DK-2800 Denmark.